THE EFFECT OF SHEAR FORCE ON MICROSTRUCTURE AND MECHANICAL PROPERTY OF EPOXY/CLAY NANOCOMPOSITE

By

TAK-KEUN OH

A THESIS PRESENTED TO THE GRADUATE SCHOOL
OF THE UNIVERSITY OF FLORIDA IN PARTIAL FULFILLMENT
OF THE REQUIREMENTS FOR THE DEGREE OF
MASTER OF SCIENCE

UNIVERSITY OF FLORIDA

2004

This document is dedicated to my parents and fiancé who helped me to finish my master degree in the University of Florida.

ACKNOWLEDGEMENTS

I would like to acknowledge my advisor, Dr. Hassan El-Shall, for giving me the opportunity to pursue a broad range of scientific explorations. His hard work and attention to detail were excellent example during my studies. Dr. Charles Beatty additionally deserves acknowledgement for enriching me about nanocomposites. I also would like to thank Dr. Abbas A. Zaman and Dr. Hassan Mervat for advising my research. Many of the advances achieved during my graduate school career would not have been possible without their assistance.

I would like to thank the National Science Foundation's Engineering Research Center for Particle Science and Technology and the Major Analytical Instrumentation Center for the use of their analytical instruments during my research endeavors.

My research was further enhanced by the support and collaboration with both past and present students and research scientists including Sangyup Kim, Dongwon Lee, Bumsu Kim, Hyun Park, Dongin Kim, Saijit Daosukho, Ajit Bhaskar, Nathan Tortorella, Kerry Siebein, Dr. Valentine Cracium and all the other students and friends who made my time satisfying at the University of Florida. Finally I would like to thank my parents, sister and my fiancé Jieun Ahn who loved and supported me while I was pursuing my master's degree.

TABLE OF CONTENTS

Page

LIST OF TABLES

Table page

LIST OF FIGURES

Figure page

Abstract of Thesis Presented to the Graduate School
of the University of Florida in Partial Fulfillment of the
Requirements for the Degree of Master of Science

THE EFFECT OF SHEAR FORCE ON MICROSTRUCTURE AND MECHANICAL PROPERTY OF EPOXY/CLAY NANOCOMPOSITE

By

Tak-Keun Oh

May 2004

Chair: Hassan El-Shall
Major Department: Materials Science and Engineering

Smectite clays [montmorillonite and bentonite] are organically modified with dodecylammonium chloride [$CH_3(CH_2)_{11}NH_3^+ \cdot Cl^-$] to investigate the effect of intergallery spacing depending on the property of clay minerals. X-ray diffraction (XRD) and Fourier transform infrared spectroscopy (FT-IR) were used to analyze the effect of cation exchange on clay surface and the exfoliation phenomenon of clay interlayer. In this research, the effect of shear force on the properties of epoxy-clay nanocomposite is also investigated. The morphology and intergallery spacing were investigated by SEM, TEM and XRD.

From the experimental results, the surface modification of clay minerals by dodecylammonium chloride shows the different increase in distance between silicate layers depending on clay minerals. Variables such as shear force and clay loading do not affect intergallery spacing of epoxy-clay nanocomposites. However, the reduced aspect ratio of silicate layers was affected by shear force. The improved tensile modulus and

thermal stability were evidenced by increasing clay-loading amounts of epoxy-clay nanocomposite

CHAPTER 1
INTRODUCTION

Polymer nanocomposites containing layer-structured, inorganic nanoparticles (clay) have been extensively researched since the Toyota research group[1-3] reported the greatly improved tensile properties and the enhanced heat distortion temperature of nylon-6 nanocomposites. In general, the dispersion of clay particles in the polymer matrix can result in the formation of three general types of composites: (a) conventional composites; the clay fraction in conventional clay composites plays little or no functional role and acts mainly as a filling agent for economic considerations, (b) intercalated nanocomposites; it is formed when one or a few molecular layers of polymer are inserted into the clay galleries with a fixed interlayer spacing, (c) exfoliated nanocomposites; the individual 10 □-thick silicate layers are dispersed in the polymer matrix and segregated from one another, and the gallery structures are completely destroyed. Both intercalated and exfoliated nanocomposites offer some special physical and mechanical properties compared to the conventional composites.[4, 5]

The *in-situ* polymerization of pre-polymers in organoclay galleries has been especially successful for the preparation of exfoliated clay nanocomposites of polyimide, unsaturated polyester,[6, 7, 8] polystyrene,[9] polypropylene[10] and epoxy [4, 5, 11-16] matrixes. Nanoscale layered clays with very high aspect ratio and high strength can play an important role in forming effective polymer nanocomposites due to their intercalation chemistry. Montmorillonite has been particularly important in polymer nanocomposites.

Montmorillonite is a crystalline 2:1 layered clay mineral in which a central alumina octahedral sheet is sandwiched between two silica tetrahedral sheets.[11]

Epoxy resin is often used in integrated circuit (IC) packaging and printed circuit boards (PCBs), such as in pin grid array packaging, ball grid array packaging and multiple moduli. To improve the thermal and mechanical properties, inorganic material such as clay is used as an additive in the epoxy resin.[17] And epoxy nanocomposite are also being utilized for wide range of applications including coating, automotive and aerospace industry.[16]

Generally, inorganic materials have neither good interaction with organic polymers to achieve good dispersion nor adequate adhesion. Surface modifications have been commonly used to achieve a better interaction of clay surface to a polymeric matrix. Ion exchange of the Na^+ or Ca^{2+} gallery cations in the pristine minerals by alkylammonium ions is generally chosen to modify the clay interlayer from hydrophilic to hydrophobic and to reduce the physical or electrostatic bonding force of clay interlayer because it leads to a favorable formation of nanocomposite and to exfoliate the interlayer of clay by several researchers.[19, 20] Much research was performed regarding the cationic surfactant, such as the effect of chain length and types of surfactant.[15]

On the processing side, Vaia[18] have suggested that the degree of exfoliation could be improved through the aid of conventional shear devices. They assumed that the individual plates peel apart through a combination of shear and diffusion of polymer chains in the organoclay gallery, as schematically shown in Figure 1-1. These authors assume the platelet on the top or bottom of a stack is able to bend away from others in the stack as the polymer chains seek to wet or make contact with the organoclay surface. As

shear force is applied, the solution becomes more viscous with the dispersion of clay particles. At higher clay content, the viscosity increases even further and it is assumed that the extra shear force generated by high viscosity would increase the basal spacing of clay platelets in the epoxy resin. It is therefore suggested that the shear mixing provides good dispersion of clay nanoparticles including intercalation and exfoliation for the shear force and residence time.[18]

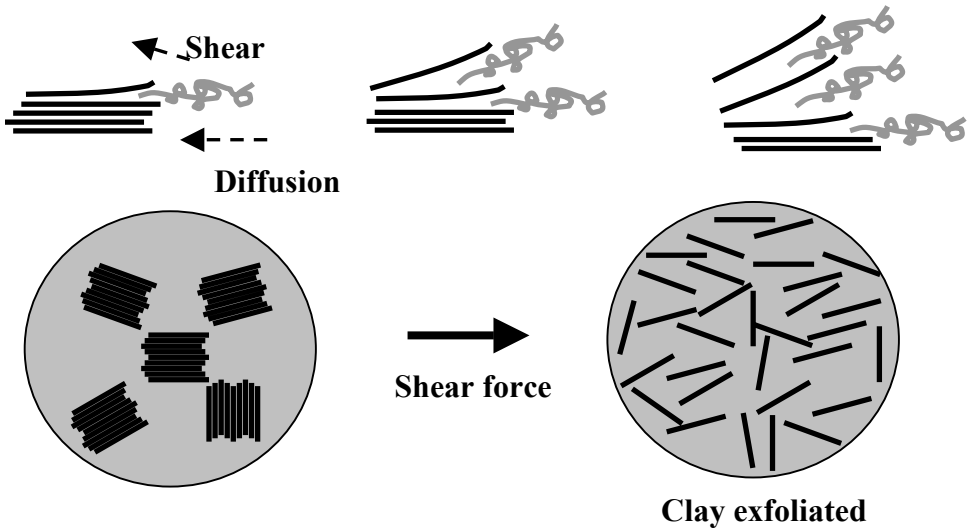

Figure 1-1. Schematic mechanisms of clay platelets intercalation/exfoliation in the epoxy matrix by shear mixing. Individual platelets peel apart from stack of the clay layers

Several investigations of the effect of shear force on properties of thermoplastic-nanocomposites have been reported to use shear device such as extruders, mixers and ultra-sonicators.[18] however, thermoset plastics are not suitable for such shear devices. Therefore, the shear force effect onto nanocomposite using thermoset plastics has not been studied extensively. Neverthrless, shear force is an important process parameter for synthesis polymer-clay nanocomposite. In this study, clay/epoxy nanocomposites were prepared by using different levels of mixing speed to investigate the effect of shear force,

clay loading and mixing time on intercalation/exfoliation using mechanical mixer. The shear force was controlled by varying the rpm [revolutions per minutes] of the rotor, ranging from 400 ~ 1000. The thermal, morphological and mechanical properties were studied with respect to the exfoliation/intercalation.

CHAPTER 2
LITERATURE REVIEW

2.1 Nanocomposites

Polymer nanocomposites are commonly defined as the combination of a polymer matrix resin and nanometer size range inclusions. The nanoparticles have at least one characteristic length scale that is of the order of nanometers and can range from essentially isotropic to highly anisotropic needle-like to sheet-like elements. Uniform dispersion of these isotropic and anisotropic nanoscopically-sized particles can lead to large interfacial area between the constituents.[21-23]

The nanocomposite chemistry with polyamide 6 pioneered by Toyota Central Research and Development has been extended in recent years to other thermoset and thermoplastic polymers. Although polymer-exfoliated clay nanocomposites are relatively difficult to prepare, the organocation modification approach has proven to be very successful for the design of other engineering polymer-clay nanocomposites.[18, 24-27]

2.1.1 Types of Nanocomposites

From a structural point of view, polymer – clay composites can be classified into ”conventional composite,” “intercalated nanocomposite” and “exfoliated nanocomposite.”

In a conventional composite (Figure 1A), there is no intercalation of polymer into the intergallery of nanoparticles when clay nanolayers are mixed with the polymer. An improvement in modulus is generally achieved in conventional clay composite, but this

reinforcement benefit is usually accompanied with a sacrifice in other properties, such as strength or elasticity.

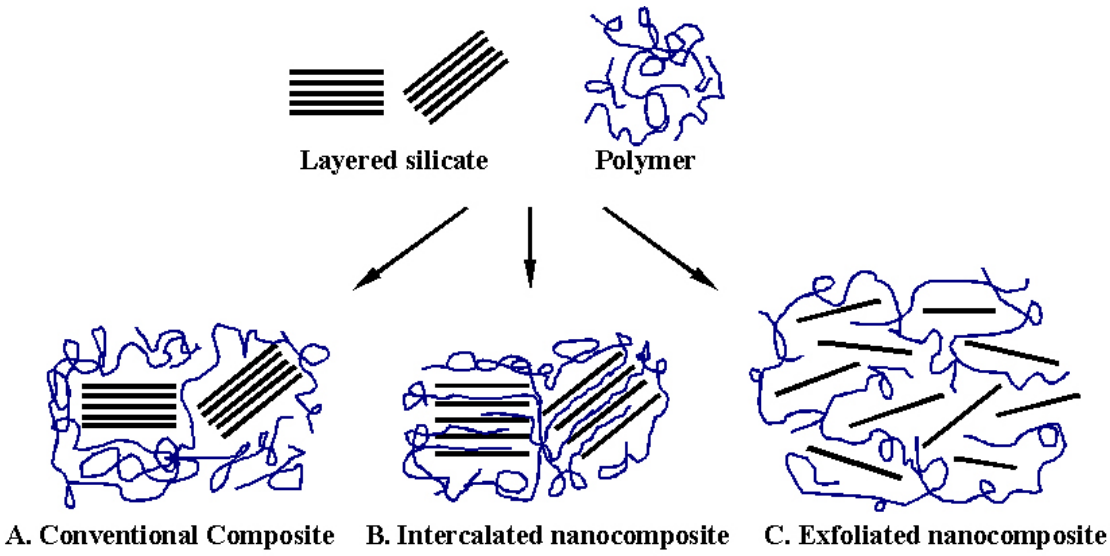

Figure 2-1. Scheme of different structure of composite arising from the intercalation of layered silicates and polymers: A) phase separated microcomposite, B) intercalated nanocomposite and C) exfoliated nanocomposite

Intercalated nanocomposites (Figure 1B) are formed when a single (and sometimes more than one) extended polymer chain is intercalated between the clay galleries resulting in a well ordered multi-layer morphology built up with alternating polymeric and inorganic layers.

When the silicate layers are completely and uniformly dispersed in a continuous polymer matrix, exfoliated nanocomposites (Figure 1C) are obtained. Exfoliated nanocomposites show greater phase homogeneity than intercalated nanocomposites. Each nanolayer in an exfoliated nanocomposite contributes fully to interfacial interactions with the matrix.[28]

2.1.2 Epoxy-Clay Nanocomposite

Akelah et al[29] have investigated the use of epoxyphilic montmorillonites for epoxy nanocomposite formation. The onium ion in these montmorillonites contained either

carboxylic acid anhydride, phenolic, hydroxyl, amine or amine functionality for reaction of an amine-cured epoxy formulation, X-ray diffraction result indicated that extensive gallery swelling occurred for both the uncured and the cured epoxy-amine-epoxyphilic clay mixtures. They showed the curing rate of the epoxy was faster in the extragallery regions of the clay than in the Na^+-occupied galleries, thus allowing most of the intragallery components to migrate out of the galleries prior to becoming crosslinked.

Messersmith and Ginannelis[30] used an epoxyphilic clay to prepare glassy epoxy nanocomposites by dispersing an ethoxylated onium ion exchanged montmorillonite in epoxy resin and curing in the presence of nadic methylanhydride, benzyldimethylamine or boron trifluoride monoethylamine at 100-200℃. Interlayer spacings of 100Å or more were observed. It is important to emphasize that the epoxyphilic functional groups on the quaternary ammonium ion modifiers used both by Akelah[29] and by Messersmith and Giannelis[30] play an important role in forming exfoliate clay nanocomposites.

T.J. Pinnavaia and T. Lan[31] have synthesized epoxy-clay nanocomposites by in-situ intragallery polymerization, exfoliating organoclays in an epoxy thermosetting process. They observed that the addition of the crosslinking agent m-phenylendiamine (mPDA) to epoxide-clay mixtures at room temperature resulted in no change intergallery spacing. However, upon initiating crosslinking at elevated temperatures, significant changes in clay intergallery spacing were shown. The chain length of gallery cations, the clay layer charge density and acidity of gallery cations govern the extent of silicate layer separation.

X. Kornmannm[32] synthesized epoxy-clay nanocomposites. Prior to curing reaction, the epoxy resin was mixed with desired amount of octadecylammonium exchanged montmorillonite at 75℃ for several hours. A stoichiometric amount of the diamine-

curing agent was added. All samples were cured 3 hours at 75℃ and post-cured either 3 hours at 160℃ or 12 hours at 110℃ to reach full cure. The result showed that delamination of the organoclay in an epoxy system is dependent on the swelling duration as well as the nature of the curing agent and the cation exchange capacity of the clay. Furthermore, the curing agent needs to have a good solubility with the clay as well as a sufficiently low reactivity so that the intrergallery polymerization can exfoliate the clay.

2.1.2.1 Tensile Properties

Wang and Pinnavaia[33] have obtained useful insights of mechanical behavior into the nature of polymer-clay nanocomposites from tensile test. The authors prepared epoxy-magadiite nanocomposite prepared by using long chain secondary (C18A1M-), tertiary (C18A2M-) and quaternary (C18A3M-) alkylammonium ion, as well as primary (C18A-) onium ion. The reinforcement effect is dependent on the extent of silicate nanolayer separation and clay loading amount. A comparison of tensile properties for the epoxy-magadiite nanocomposites prepared from C18A1M-, C18A2M-, and C18A3M-magadiite. The tensile strengths of the microscopically homogeneous intercalated and exfoliated magadiite nanocomposites are superior to conventional composites with macroscopic homogeneity. Clearly, the tensile properties improve with increasing degree of nano-layer separation.

Asma Yasmin[16] made epoxy-clay nanocomposite by shear mixing and investigated the stress-strain behavior. The elastic modulus of nanocomposites is found to increase with increasing concentration of clay and a maximum of 80% improvement is observed for an addition of 10 wt.% of clay. The decreasing rate of elastic modulus improvement with higher clay content is described by the inevitable aggregation of clay particle. The

result also shows lower or no improvement in tensile strength of nanocompositea over pure epoxy due to the clustering of nanoparticles and/or to the occasional occurrence of nano- to micro-size voids in the microstructure. And also they found higher tensile strength with degassed nanocomposite.

2.1.2.2 Thermal Stability

Wang and Pinnavaia[33] compared the TGA curves for an exfoliated nanocomposite prepared from C18A1M-magadiite and an intercalated nanocomposite prepared from C18A3M-magadiite. The lower temperature weight loss for the intercalated C18A3M-magadiite nanocomposite is indicative of the decomposition of the quaternary alkylammonium cations on the magadiite basal planes, because an analogous weight loss is observed for pristine C18A3M-magadiite. In comparison, the TGA curves for the exfoliated C18A1M-magdiite nanocomposite does not show a similar low temperature loss for the decomposition of surface onium ions, verifying that the secondary onium ions are indeed incorporated into the polymer network.

Wei Feng[34] compared T_g of Bis (2-hydroxylethyl) methyl tallow ammonium montmorillonite-epoxy nanocomposite (TCN) with that of Tolylene 2, 4-diisocyanate montmorillonite nanocomposite (TDI-BA). Their result shows that the glass transition temperature increases with increasing the amount of organoclay. This suggests the layered silicate hinder the motion of molecules in the epoxy network at least in the vicinity of the silicate surface. It also indicate the TDI-BA modification of the 1.34 TCN organoclay results in higher values of T_g in comparison with T_g values obtained with 1.34 TCN organoclay. This is attributed to enhance molecular interactions at the interface between layered silicates and epoxy matrix promoted by the hydroxyl groups of the BA, which are believed to participate to the formation of the epoxy matrix network.

2.1.2.3 Chemical Stability and Solvent Resistance

Exfoliated epoxy-clay nanocomposites exhibit not only superior mechanical properties but also exceptional chemical stability and solvent resistance. For instance, the uptake of methanol and propanol is faster for pristine polymer than for the nanocomposite materials. In the case of methanol, the equilibrium absorption after 30 days is almost equal to that of the pristine polymer. However, the pristine sample after being submerged 30 days in methanol was rubbery, whereas the composite material appeared unaffected by the solvent. After 50 days in propanol, the pristine polymer absorbs 2.5 times more than the nanocomposite. And at this time the pristine sample began to crack and break up, whereas the shape and texture of the nanocomposite sample appeared unchanged. Toluene absorption by the pristine sample was 5 times greater than the amount absorbed by the 5 wt.% clay loading nanocomposite.

2.1.2.4 Optical Transparency

N Salahuddin[13] shows the transparency of epoxy-clay (60 wt.% MMT) nanocomposite. The compressed molded samples are transparent as is ordinary epoxy resin. This fact is explained by the molecular level dispersion of montmorillonite of a size smaller than the wavelength of visible light. This result is very encouraging since improved or novel properties of the composite material would be expected with homogeneous dispersing size going down to such a nanometer level.

2.1.3 Types of polymers used for nanocomposites preparation

A Polymer nanocomposite containing layer-structured inorganic nanoparticle was first introduced by researchers from Toyota who discovered the possibility to build a nanocomposite from polyamide 6 and organophilic clay. Numerous other researchers later used this concept for nanocomposites based on unsaturated polyester, poly (ε-

caprolactone), poly (ethylene oxide), polystyrene, polyimide, etc. Those materials were produced either by melt intercalation of thermoplastics or in situ polymerization.

2.1.3.1 Nylon 6-Clay Nanocomposite

Arimitsu Usuki[35] synthesized nylon 6-clay hybrid materials using four types of clay minerals: montmorillonite, saponite, hectite and synthetic mica. The mechanical properties of their injection-molded specimens were measured according to ASTM. Nylon 6-clay hybrid using montmorillonite was superior to the other hybrids in mechanical properties. This results from the difference in the interaction between nylon molecules and silicates in the hybrids.

They also found that montmorillonite cation exchanged for 12-aminolauric acid was swollen by ε-caprolactam to form a new intercalated compound. Caprolactam was polymerized in the interlayer of montmorillonite, a layered silicate, yielding a nylon 6-clay hybrid (NCH). The silicate layers of montmorillonite were uniformly dispersed in nylon 6. The carboxyl end groups of 12-aminolauric acid in 12-montmorillonite initiated polymerization of ε-caprolactam, and as 12-montmorillonite content become larger, the molecular weight of nylon was reduced. The difference between the carboxyl and the amino end groups was attributed to ammonium cations ($-NH_3^+$) of nylon molecules, because the difference agreed with the anion site concentration of the montmorillonite in NCH. It is suggested that the ammonium cations in nylon 6 interact with the anions in montmorillonite.

2.1.3.2 Polyimide-Clay Nanocomposite

Kazuhisa Yano[6] investigated the effect of the size of clay minerals to the properties of polyimide-clay hybrid. Hectrite, saponite, montmorillonite, and synthetic mica were

used as clay minerals. This clay consists of stacked silicate sheets about 460 Å (hectrite), 1650 Å (saponite), 2180 Å (monrmorillonite), and 12300 Å (synthetic mica) in length, 10 Å in thickness. The greater the length of clay, the more pronounced increase in properties. In the case of polyimide-mica nanocomposite, only 2 wt.% addition of synthetic mica brought permeability coefficients of water vapor to value less than one-tenth of that of ordinary unfilled polyimide, and thermal expansion coefficient was lowered at the level of 60% of the original one.

2.1.3.3 Unsaturated polyester-clay Nanocomposite

Suh D.J.[36] investigated the property and formation mechanism of unsaturated polyester-layered silicate nanocomposite based on the fabrication methods. Sampeles were prepared by two different mixing methods. The first method, simultaneous mixing, is similar to the method used for preparing the conventional unsaturated polyester and filler composite. The second method is sequential mixing, a new approach for preparing unsaturated polyester-layered nanocomposite. Mixture of the UP and organophilic-treated MMT are prepared and styrene monomer was added to the pre-intercalated UP/MMT with varying mixing time. The styrene monomer diffuses easier than uncured UP chains. This may generate higher styrene monomer concentration in the MMT gallery than any other part in a simultaneous mixing system.

2.1.3.4 Polystyrene-Clay Nanocomposite

Tseng Chen-Rui[37] prepared syndiotactic polystyrene-modified clay nanocomposite using polymer intercalation from solution. The experimental result indicate that s-PS chains can intercalate more efficiently into the silicate layers when clay is pretreated with CPC (cetyl pyridium chloride) surfactant.

Jeffrey W[38] investigated flammability properties of polypropylene and polystyrene nanocomposite. They observed that an intercalated PS-fluorohectorite nanocomposite is ineffective at reducing the flammability of PS, possible due to the large aspect ratio of flurohectorite. However, they found that an antagonistic interaction between high processing temperatures and the alkylammonium MMT, which causes an increase in the polydispersity in PS-MMT nanocomposites during processing. Their view of the general nanocomposite flame retardant mechanism is that a high-performance carbonaceous-silicate chars builds up on the surface during burning; this insulates the underlying material and slows the mass loss rate of decomposition products.

2.1.3.5 Poly (ethyleneterephathalate) (PET)-Clay Nanocomposite

Ke Y.[39] prepared poly (ethyleneterephathalate) (PET)-clay nanoscale composites by intercalation, followed by in-situ polymerization. They made refined clay into slurry first, forming solution with intercalated reagent. The obtained clay, called treated clay, directly reacts with PET monomers in an autoclave. They found that the exfoliated clay particles play a nucleating role and have strong interactions with PET molecular chains. Thus, the nano-PET properties are enhanced compared with the PET itself. The other reason may possibly be the relatively weak interface formed between clay particle and the matrices of PET resulting from the agglomerated particles.

2.1.3.6 Polypropylene (PP)-Clay Nanocomposite

Yoo Y.[40] prepared a polypropylene (PP)-clay nanocomposite through the ultrasonic melt intercalation by mixing 5wt% organophillic clay, Cloisite ®20A (Southern Clay Products Inc.) with three types of PP in internal mixer (Rheomix 600, Haake Rheocord 90). During mixing, the mixture was exposed to the ultrasonic wave. They found that

increasing the sonification time on nanocomposites, storage modulus was improved, but the degree of degradation of neat PP was increased.

2.2 Clay

The term “clay” refers to any materials which exhibits a plastic behavior when mixed with water, while “clay mineral” refers to materials which have a layer structure or a structure substantially derived from or containing major features of such layer structures. For example, clay minerals are kaolinite, illite, and smectite but not, micas, talc, and pyrophyllite which occur in much larger particle size.

As the name indicates, phyllosilicate (from the Greek, phyllon, a leaf, as in a leaf of a plant) minerals are layered structures. That is, the atomic arrangement is such that there are easily recognizable quasi two-dimensional fragments, strongly bonded internally, which are stacked one on top of the other with a much weaker bonding between the layers.[41]

2.2.1 Types of Layered Silicates

There are several aspects of the overall crystal structure of phyllosillicates that are important in determining the properties of these materials and their nomenclature. Table 2-1 shows a scheme of phyllosilicates.

The commonly used layered silicates for the preparation of nanocomposites belong to the same general family of 2:1 layered or phyllosilicates. Their crystal structure consists of layers made up of two tetrahedral coordinated silicon atoms fused to an edge-shared octahedral sheet of either aluminum or magnesium hydroxide. The layer thickness is around 1 nm, and the lateral dimensions of these layers may vary from 30 nm to several microns or larger, depending on the particular layered silicate. Stacking of the layers leads to a regular van der Waals gap between the layers called the interlayer or

gallery. Isomorphic substitution within the layers (for example, Al^{3+} replaced by Mg^{2+} or Fe^{2+}, or Mg^{2+} replaced by Li^{1+}) generated negative charges that are counterbalanced by alkali and alkaline earth cations situated inside the galleries.

Table 2-1. Classification scheme for phyllosilicates related to clay minerals

Type	Group		**Species***
1:1	**Kaolinete-serpentine**	**Kaolinites** **Serpentines**	**Kaolinite, Halloysite,** **Antigorite, Chrysotile**
2:1	**Pyrophyllite-talc**	**Pyrophyllites**	**Pyrophyllites** **Talc**
	Smectite or Montmorillonite-saponite	**Smectites or Montmorillonites** **Smectites or Saponites**	**Montmorillonite,** **Beidellite, Nontronite** **Saponite, Hectorite,** **Sauconite**
	Vermiculite	**Vermiculites** **Vermiculites**	**Dioctahedral Vermiculite** **Trioctahedral Vermiculite**
	Mica	**Micas** **Micas**	**Muscovite, Paragonite** **Biotite, Phlogopite**
	Brittle Mica	**Brittle Micas** **Brittle Micas**	**Margarite** **Clintonite**
2:1:1	**Chlorite**	**Chlorites** **Chlorites** **Chlorites**	**Donbassite** **Sudoite** **Pennine, Clinochlore**

This type of layered silicate is characterized by a moderate surface charge known as the cation exchange capacity (CEC), and generally expressed as mequiv/100gm. This charge is not locally constant, but varies from layer to layer, and must be considered as an average value over the whole crystal.[28]

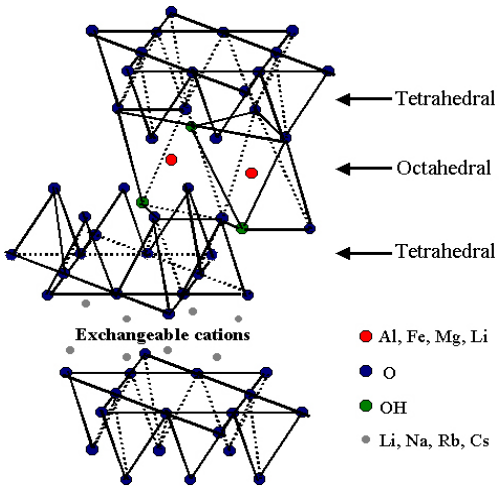

Figure 2-2. Structure of 2:1 phyllosilicates

MMT (montmorillonite), hectorite, and saponite are the most commonly used layered silicates. Layered silicates have two types of structure: tetrahedral-substituted and octahedral substituted. In the case of tetrahedrally substituted layered silicates the negative charge is located on the surface of silicate layers, and hence, the polymer matrices can react and interact more rapidly with these than with octahedral-substituted material. Details regarding the structure and chemistry for these layered silicates are provided in Figure 2-2.

2.2.2 Organically Modified Layered Silicates

The physical mixture of a polymer and layered silicate may not form a nanocomposite. This situation is analogous to polymer blends, and in most cases separation into discrete phases takes place. In immiscible systems, which typically correspond to the more conventionally filled polymers, the poor physical interaction between the organic and the inorganic components leads to poor mechanical and thermal properties. In contrast, strong interactions between the polymer and the layered silicate in PLS nanocomposites lead to the organic and inorganic phases being dispersed at the nanometer level. [43-48]

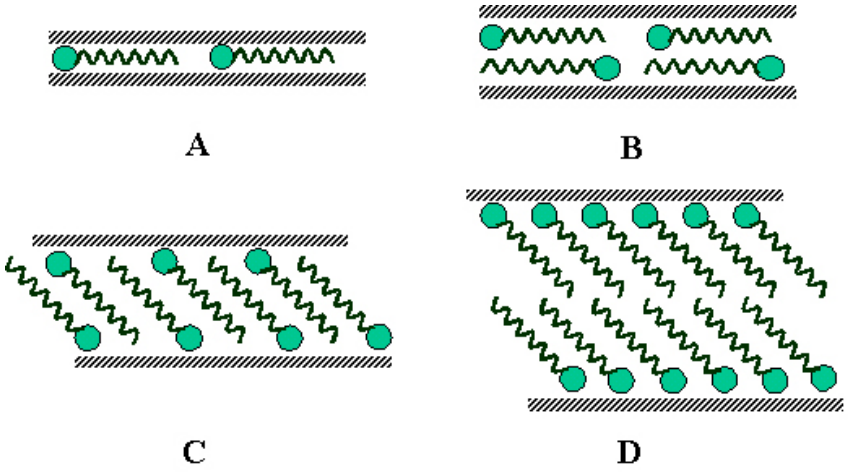

Figure 2-3. Arrangements of alkylammonium ions in mica-type layered silicates with different layer charges. A) lateral monolayer, B) lateral bilayer, C) paraffin-type monolayer and D) paraffin-type bilayer

Pristine layered silicates usually contain hydrated Na^+ or K^+ ions.[49] Obviously, in this pristine state, layered silicate is only miscible with hydrophilic polymers, such as poly ethylene oxide (PEO)[50], or poly vinyl alcohol (PVA)[51]. To render layered silicates miscible with other polymer matrices, one must convert the normally hydrophilic silicate surface to an organophilic one, making the intercalation of many engineering polymers possible. Generally, this can be done by ion-exchange reactions with cationic surfactants including primary, secondary, tertiary and quaternary alkylammonium or alkylphosphonium cations. Alkylammonium or alkylphosphonium cations in the organosilicates lower the surface energy of the inorganic host and improve the wetting characteristics of the polymer matrix, and result in a larger interlayer spacing. Additionally, the alkylammonium or alkylphosphonium cations can provide functional groups that can initiate the polymerization of monomers to improve the strength of the interface between the inorganic and polymer matrix [52, 53].

Depending on the packing density, temperature and alkyl chain length, the chains were thought to lie either parallel to the silicate layers forming mono or bilayers, or

radiate away from the silicate layers forming mono or bimolecular arrangements (Figure 2-3).

2.3 Epoxy Resin

The first attempts at commercializing epoxy resins were made in 1927 in the USA but the two people credited with developing epoxy resins from bisphenol 'A' and epichlorohydrin, which is by far the largest class of epoxy resins in commercial usage today.

2.3.1 Epoxy Resin based in Bisphenol 'A' and Cross-link Reaction

Bisphenol 'A' based epoxy resins are produced by the condensation of epichlorohydrin(ECH) with diphenylpropane (DPP) (bisphenol 'A') in the presence of catalyst as shown in Figure 2-4.The great majority of epoxy resins are used in crosslink systems, which also referred to as curing. Epoxy resins can either crosslink at room temperature or at elevated temperatures.

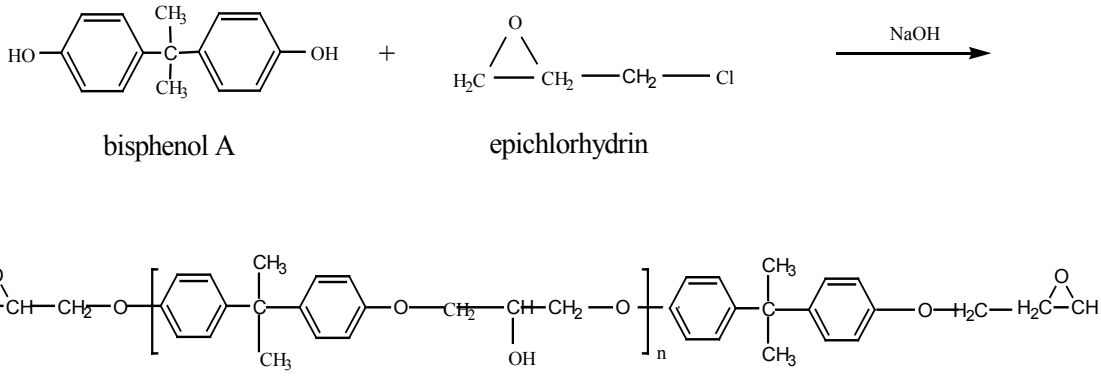

Figure 2-4. Production of Epoxy Resin

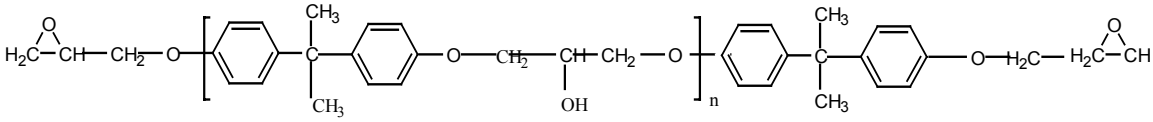

Epoxy resin

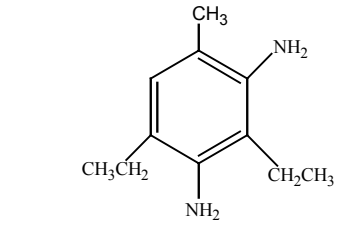

Diethyltoluenediamine

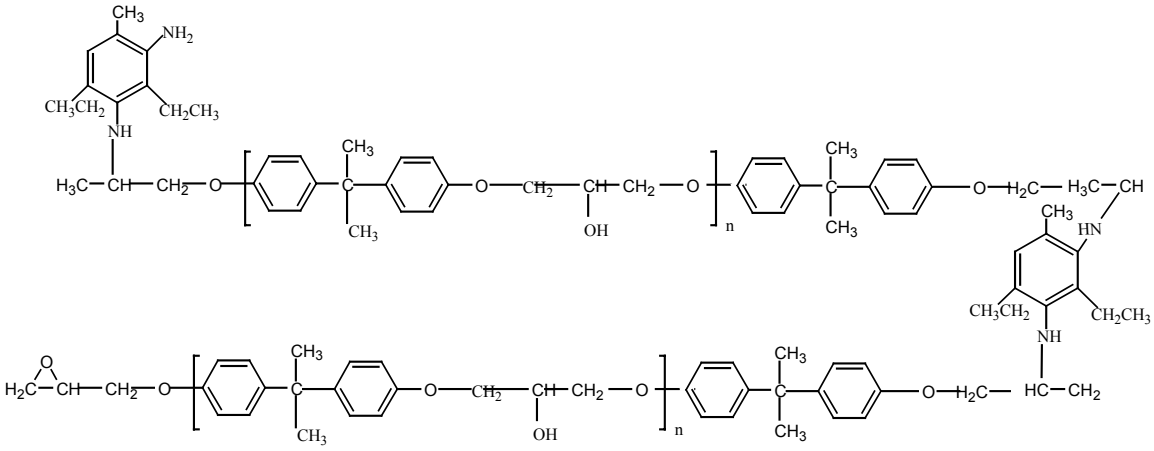

Figure 2-5. Crosslinking reaction between epoxy resin and diethyltoluenediamine

Amines are universally used as curing agents for two pack epoxy systems. They either catalyze the curing reaction, as is the case for tertiary amines, or participate in the curing reaction, as is the case for primary and secondary amines. The epoxy curing reactions normally utilize either the epoxy group of the epoxy resin or the secondary hydroxyls, even if they are formed as part of the reaction of the epoxy group. For the outstanding chemical resistance attributed to epoxy containing systems, it is essential that a good degree of reaction and consequently a good degree of cure be achieved. Figure 2-5 shows the crosslink reaction of epoxy resins with diethyltoluenediamine (DETDA), which is used in this research.

2.3.2 Uses of Epoxy

Epoxy resins have been commercially available for more than forty years and are used in one of the most diverse range applications in the modern world. They are mostly

used in the surface coating industry. They are also used in both thermal and ambient cure applications in industries such as aerospace, civil engineering, automotive, chemical, electrical, marine, leisure and many others.

Epoxy is used with all kinds of reinforcement, but most commonly together with carbon fibers, since the combination offers an attractive blend of properties and cost. Common applications include

- High performance racing vehicle and yachts
- Aircraft control surface and skins
- Space craft
- Pressure vessel
- Launch tubes for portable grenade launchers

CHAPTER 3
EXPERIMENTAL AND CHARACTERIZATION METHOD

3.1 Materials

For modification of a hydrophilic natural clay to organophilic clay, natural clay (cloisite Na+; Southern clay product in USA) was used. This Cloisite Na+ is montmorillonite. Four different types of bentonite were also used for this modification. These bentonites were supplied by Central Metallurgical R&D Institute (in Egypt).

For preparation of nanocomposite, the cloisite 30B, which is an organically modified montmorillonite with a methyl tallow bis-2-hydroxyethyl quaternary ammonium, was used as a reinforcement clay nanoparticle. This cloisite 30B was received from Southern Clay Products (in USA). The physical properties of Cloisite 30B are shown in Table 3-1.

Table 3-1. Physical properties of cloisite 30B (modified montmorillonite)

Physical Properties	Cloisite 30B
Color	Off White
Density,(g/㎤)	1.98
d-spacing (d_{001})	18.5
Aspect ratio	200~1000
Surface area (㎡/g)	750
Mean particle size	6

The epoxy resin was the diglycidyl ether of bisphenol A (DGEBA, epoxide equivalent weight = 178g, EPON 828) and Diethyltoluenediamine (EPI-CURE W) was used as a curing agent. These epoxy resin and curing agent were provided from Shell Chemicals (in USA).

3.2 Surface Modification

Five grams of each clay mineral [montmorillonite (cloisite Na^+), bentonite A, bentonite AA, bentonite C, and bentonite CA] were dispersed into 200㎖ of distilled water at 80℃ in the round bottom three angle necks & joint 500㎖ flask. A condenser was used for this surface modification to prevent evaporation of water. As shown in Figure 3-1, the hot plate was used for heating distilled water and silicon oil bath and thermometer were used for controlling temperature.

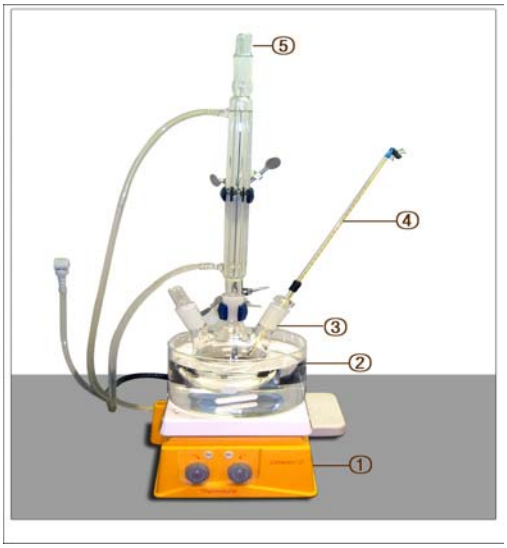

Figure 3-1. Experimental setup for clay surface modification. (1) Hot plate, (2) Silicon oil bath, (3) 500 ml Three angle necks & joint flask, (4) Thermometer, and (5) Condenser

Dodecylammonium chloride, [$CH_3(CH_2)_{11}NH_3^+ \cdot Cl^-$, MW: 221.82] was prepared by mixing 2.2182 grams of dodecylamine hydrochloride with 100㎖ of distilled water. This solution was poured in the hot clay mineral/water solution and stirred with magnetic stir bar vigorously for at 80℃ 1 hr. A white precipitate was formed, separated by centrifugation, and washed several times in hot distilled water until no chloride was detected in the filtrate by one drop of 0.1 N $AgNO_3$ solutions. Centrifugation was

preceded with Fisher Marathon 21000R centrifuge at 7000 rpm for 15 min. The resulting materials were dried in a convection oven at 80℃. The dried organic clay was grinded.

3.3 Synthesis of Epoxy-Clay Nanocomposite

The epoxy resin was mixed with a desired amount of organophilic clay [cloisite 30B] in a 2000 ㎖ beaker. A mechanical mixer [LIGHTNIN LabMaster ™ SI Mixer, model L1U08F, in IRELAND] that has A310 impeller [86 ㎜mm diameter] was used to mix the samples at different speeds (different shear forces). The onium-ion-exchanged clay was dispersed uniformly in epoxy monomer at 80℃ for 1 hr. Then, a curing agent [diethyltoluenediamine] was added into the epoxy/clay hybrid and mixed thoroughly by the mechanical stirrer. The mixtures were then degassed to remove bubbles using a vacuum oven before they were cast into a mold. Bottom, frame and top cover of mold was made from an aluminum foil covered corning micro slides [75 * 50 ㎜plain, 0.96 to 1.06 ㎜thickness]. The samples were cured in a vacuum oven for at 100℃ 10 hr.

3.4 Characterization Techniques

The change in the interlayer spacing of clay minerals [montmorillonite and bentonite] was measured using a Philips MRD X'Pert with a rotation anode and CuK_α radiation (λ = 1.5418 Å). The scanning range is from 1.05° to 9.95°. The structure of the clay was investigated at different stages during the nanocomposite synthesis. The clay particles were mounted on a sample holder with a large cavity and a smooth surface was obtained by pressing the particles with a glass plate. Analyses of organoclay swollen in the epoxy resin or in the curing agent were performed by spreading the mixture on a sample holder. The nanocomposite plates produced during the moulding process had a fairly smooth surface.

FT-IR [Fourier Transform Infrared Spectroscopy, Nicolet MAGNA 760, in USA] was used to verify the surface modification by the cationic surfactants. The sample was prepared by mixing 90% KBr and 10% clay minerals and then placing it on the disc. Transmittance was used and scans were operated from 1000 to 4000 cm^{-1} and took 124s to complete.

Differential scanning calorimetry (DSC) tests were carried out on composites using a TA Instruments SDT 2960 Simultaneous DSC-TGA analyzer. Samples were heated to 600□ at a scanning rate of 10□/min under flowing argon. The tensile test was performed on an Endura TEC ELF3200 at a 0.01 □/sec crosshead rate. Samples were prepared ~4㎜ wide, ~50㎜ length and ~1㎜ thickness in size.

The morphology of the nanocomposite was examined by JSM 6335 field emission scanning electron microscopy (SEM). Fracture surfaces of tensile specimens were coated as carbon to avoid charging and were examined at 5 □ accelerating voltage.

CHAPTER 4
RESULTS AND DISCUSSION

4.1 Clay Modification

The replacement of inorganic exchange cations with organic onium ions on the gallery surfaces of smectite clays not only serves to match the clay surface polarity with the polarity of the polymer, but also to expand the clay galleries. This facilitates the penetration of the gallery space (intercalation) by either the polymer precursors or preformed polymer. Different arrangements of the onium ions are possible depending on the charge density of clays and onium ion surfactants. If the polarity of the organoclay sufficiently matches the monomer or prepolymer, it will intercalate into the galleries, further spreading clay layers apart. Each clay mineral will show different cation exchange capability and different intergallery spacing by modification with cationic surfactants.

In this research, natural montmorillonite and four different types of bentonites were modified by dodecyl-amine hydrochloride surfactant. The alternation from hydrophilic clay to organophilic clay with cationic surfactant was vertified by FT-IR spectroscopy. Figure 4-1 shows infrared spectra of unmodified clay (montmorillonite and bentonite) and modified clays.

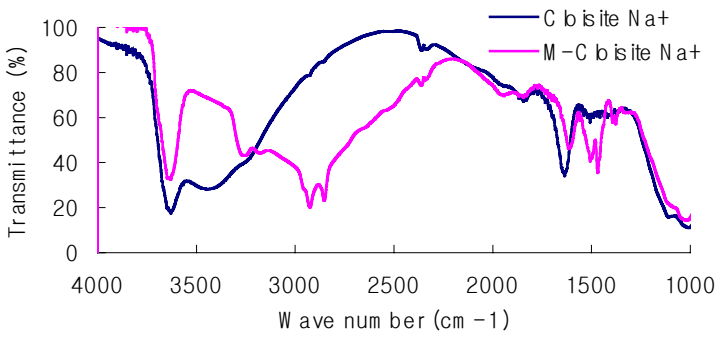
Cloisite Na+
M-Cloisite Na+
Transmittance (%)
100
80
60
40
20
0
4000
3500
3000
2500
2000
1500
1000
Wave number (cm-1)

A

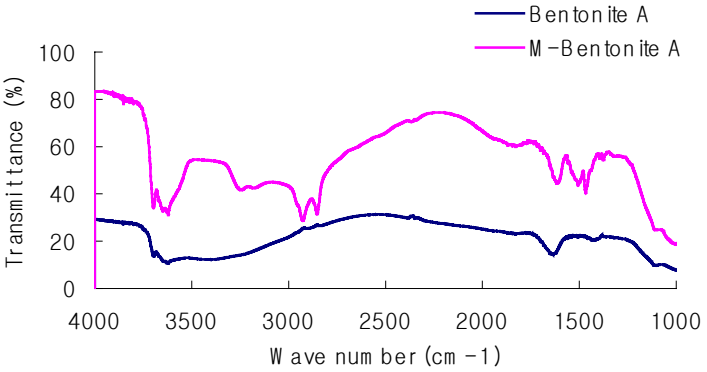
Bentonite A
M-Bentonite A
Transmittance (%)
100
80
60
40
20
0
4000
3500
3000
2500
2000
1500
1000
Wave number (cm-1)

B

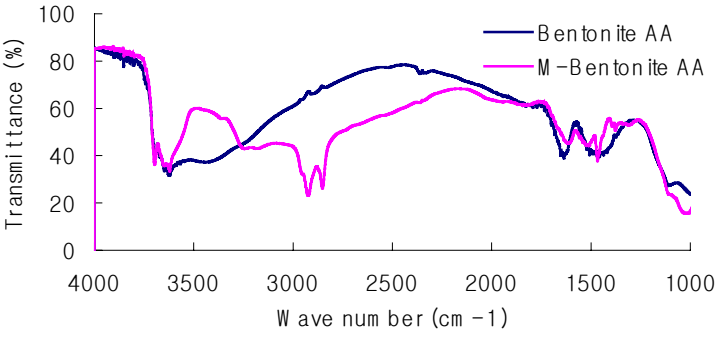
Bentonite AA
M-Bentonite AA
Transmittance (%)
100
80
60
40
20
0
4000
3500
3000
2500
2000
1500
1000
Wave number (cm-1)

C

Figure 4-1 Continued

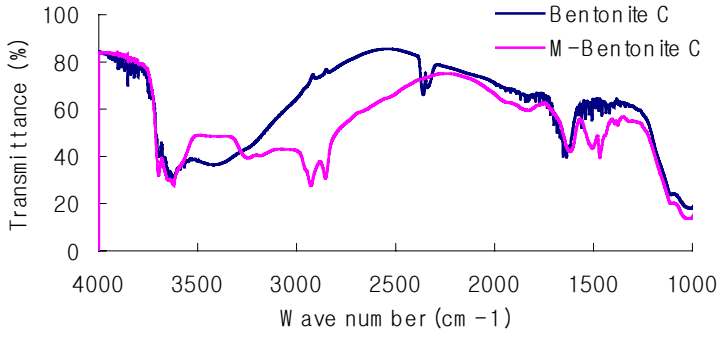

D

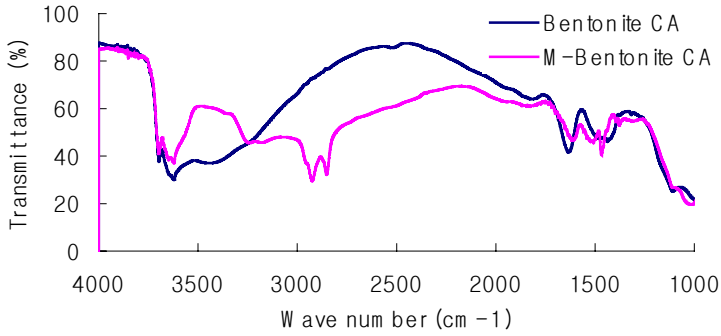

E

Figure 4-1. FTIR analysis of unmodified and modified clay minerals A) montmorillonite, B) Bentonite A, C) Bentonite AA, D) Bentonite C, and E) Bentonite CA.

The peak at 1027 cm^{-1} is associated with Si-O stretching vibrations and the peak at 3200~3700 cm^{-1} is associated with Si-OH stretching vibrations. Absorption bands, on the other hand, at 3000~2900 cm^{-1} (CH_3 stretching) and 1510~1650 cm^{-1} (NH_3^+ peak) are a consequence of the cationic surfactant [dodecyl-amine hydrochloride surfactant]. It appears that the montmorillonite and four different bentonite clay interlayers have been organically modified by dodecylammonium chloride.

Surface modification not only changes the property of surfaces but also expand the intergallery spacing. Figure 4-2 shows the XRD patterns of modified and unmodified clay (montmorillonite and four different bentonite).

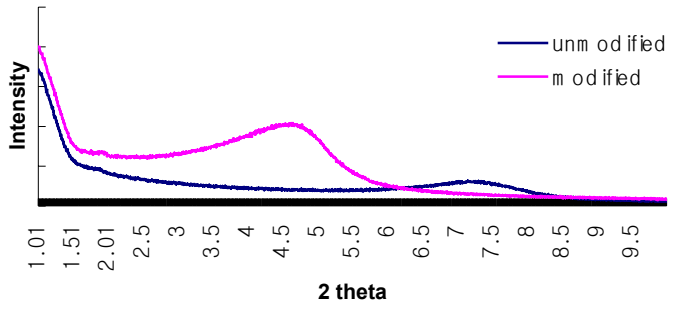

A

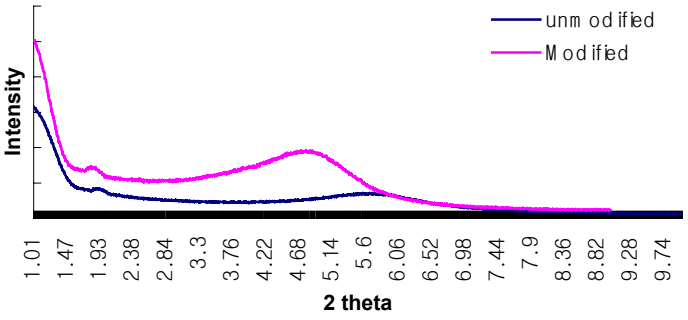

B

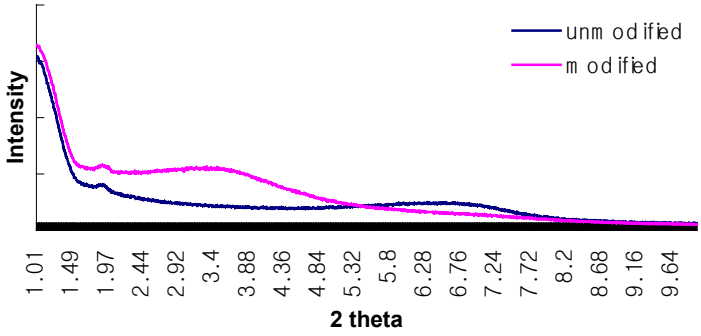

C

Figure 4-2. Continued

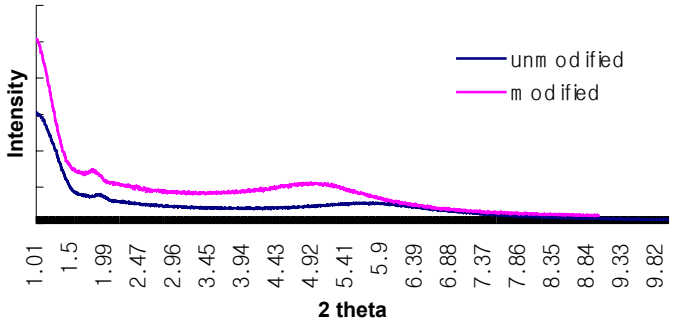

D

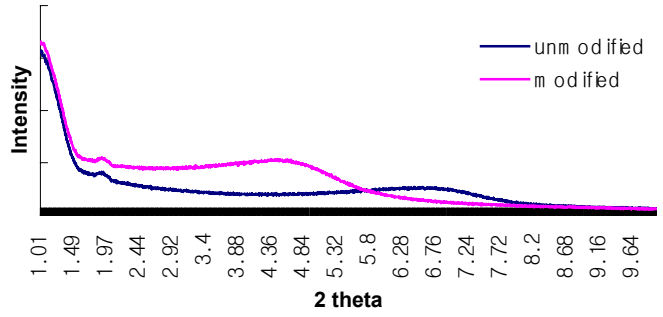

E

Figure 4-2. XRD analysis of unmodified and modified clay minerals A) montmorillonite, B) Bentonite A, C) Bentonite AA, D) Bentonite C, and E) Bentonite CA.

Every clay mineral shows a peak at 2θ = 1.9°, which is assumed to be the clay characteristic peak because it appears on unmodified clay mineral XRD data. Unmodified montmorillonite [cloisite Na+] shows a peak at 2θ = 7.295°, $d_{(001)}$ = 12.118Å. After modification the montmorillonite surface, this peak was shift to 2θ = 4.635°, $d_{(001)}$ = 19.046 Å. Intergallery spacing of montmorillonite was expanded to around 7 Å, which means cationic surfactants were exchanged with cations and changed hydrophilic surface property to organophilic. A peak of unmodified bentonite A is appeared at 2θ = 5.7111°,

$d_{(001)}$ = 15.474 Å and shifted to 2θ = 4.8°, $d_{(001)}$ = 18.41 Å by modification. This bentonite A increased the intergallery spacing to around 3Å In case of bentonite AA, this intergallery spacing increment was around 15 Å, from 2θ = 6.7847°, $d_{(001)}$ = 13.028 Å to 2θ = 3.5866°, $d_{(001)}$ = 24.634 Å. However, bentonite C and CA show 3□ [from 2θ = 5.8207°, $d_{(001)}$ = 15.183 □ to 2θ = 4.9°, $d_{(001)}$ = 18.03 Å] and 5□ [from 2θ= 6.6917°, $d_{(001)}$ = 13.209 Å to 2θ = 4.6673°, $d_{(001)}$ = 18.940 Å] increments, respectively. It seems that cation surfactants can be differently arranged depending on the cation exchange capability. The difference of intergallery spacing among the clay minerals suggests that there is different cation sufactant arrangement because of different cation exchange capability. The result shows that the expansion of intergallery spacing in bentonite AA is bigger than others. This can be interpreted that the arrangement of cationic surfactant in the bentonite AA is different from others. If more cation sites exist in the gallery, more cationic surfactant exchanged with cations in the gallery, resulting more packed arrangement of surfactant. This packed cationic surfactant can be arranged by forming bilayer. The difference among other bentonites [bentonite A, C and CA] may be attributed that the different cation exchange capabilities affect the arrangement angle of surfactant in the gallery. If intergallery spacing was expanded more, it can be assumed that epoxy resin can penetrate between the galleries easier. These XRD results reveal that clay mineral properties such as elements and CECs [cation Exchange Capabilities] were important factors to prepare the exfoliate epoxy-clay nanocomposite.

4.2 Epoxy – Clay Nanocomposites

4.2.1 Morphology

Natural Montmorillonite [Cloisite Na^+] has a negatively charged crystalline structure in which a central alumina octahedral sheet is sandwiched between two silica tetrahedral sheets. This natural montmorillonite shows a hydrophilic property. When the cation site is exchanged by cationic surfactants, a methyl, tallow, bis-2-hydroxyethyl, quaternary ammonium, the lattice spacing of clay rises and hydrophilic nature of montmorillonites changes to organophilic nature, allowing dispersion in organic solvent. The monomer of epoxy resins readily entered into the gallery of organophilic montmorillonite. X-ray diffraction (XRD) measurements can be used to characterize these gallery spacings if diffraction peaks are observed in the low-angle region: such peaks indicate the d spacing (basal spacing) of ordered-intercalated and ordered delaminated nanocomposites.

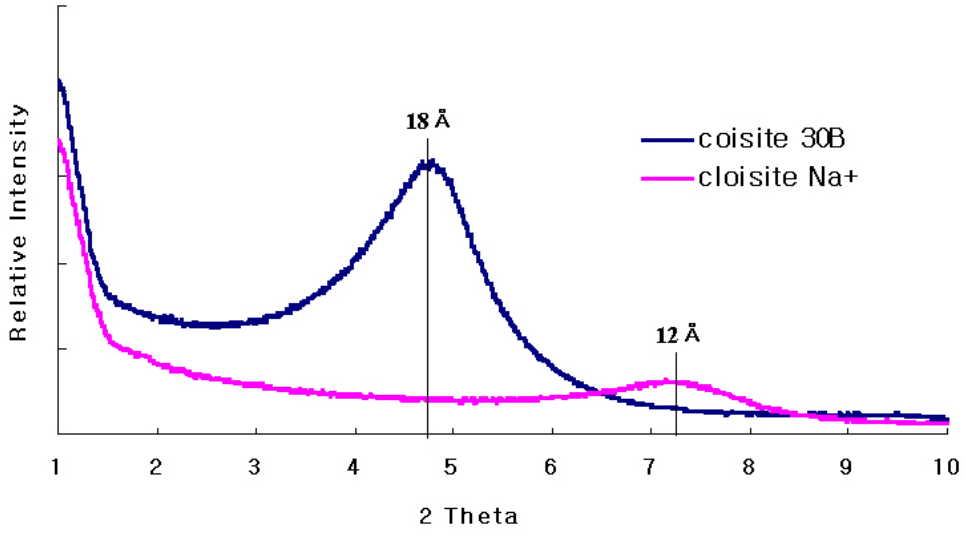

Figure 4-3. X-ray diffraction patterns of natural montmorillonite and modified montmorillonite.

Figure 4-3 shows different XRD patterns of natural montmorillonite [cloisite Na^+] and cloisite 30B [organically modified montmorillonite]. The intergallery spacing was calculated using the Bragg's equation [1],

$$\lambda = 2d \bullet \sin\theta \qquad [1]$$

The interlayer spacing of the cloisite 30B is larger than that of the cloisite Na^+; this is because the cloisite 30B contains a methyl, tallow, bis-2-hydroxyethyl, quaternary ammonium surfactant. Cloisite Na^+ and cloisite 30B [organically modified montmorillonite] show characteristic diffraction peaks at 7.3° and 4.8°, respectively. These 2θ values correspond to interlayer spacing of 12.15 Å and 18.46 Å, respectively.

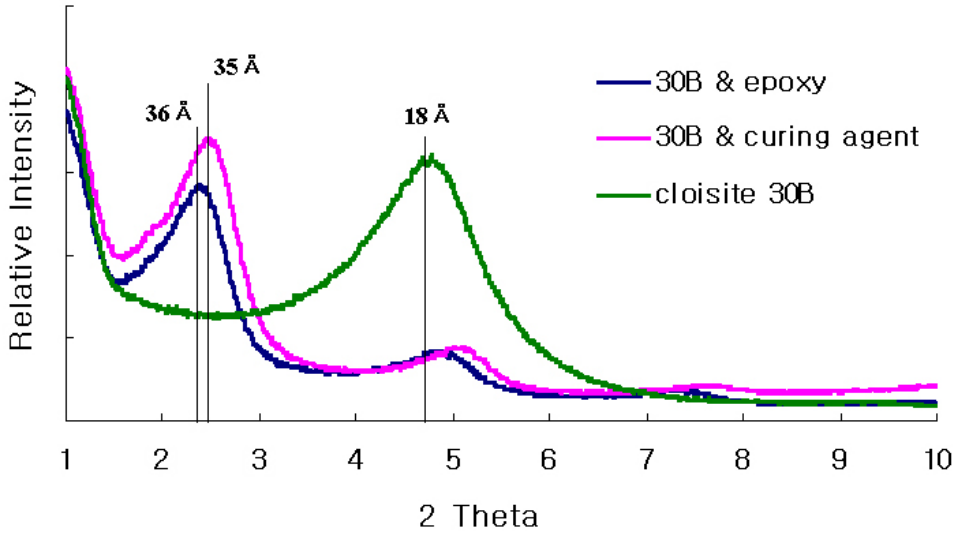

Figure 4-4. X-ray diffraction peaks of organo-montmorillonite [cloisite 30B], epoxy & cloisite 30B mixture and during agent & cloisite 30B mixture.

When an organo-montmorillonite [cloisite 30B] is mixed with epoxy, the peak was shifted to the lower angle at 2θ = 2.415°, $d_{(001)}$ = 36.57 Å and the peak of cloisite 30B and diethyltoluenediamine (DETDA) mixture appears at 2θ = 2.415°, $d_{(001)}$ = 35.11 Å in Figure 4-4. The result demonstrates the monomer of epoxy resins or a curing agent was

diffused into the galleries, resulting in the increase of the gallery spacing. The peak of organo-montmorillonite mixed with epoxy resin or curing agent which is appeared at around 5° can be explained by remaining organoclays which epoxy or curing agent didn't diffuse into the galleries.

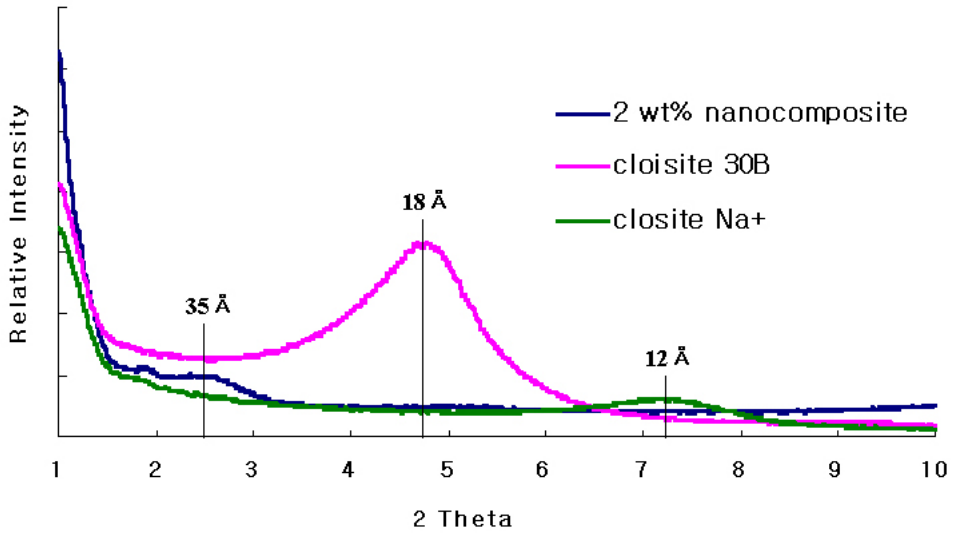

A) X-ray diffraction Peaks

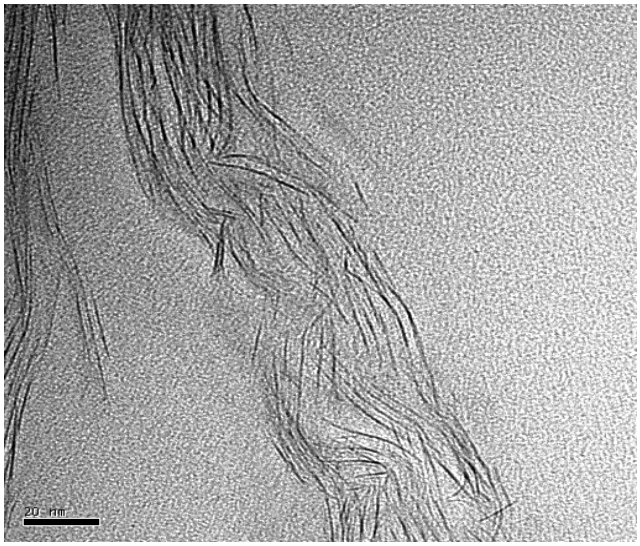

B) TEM

Figure 4-5 A) Compared X-ray diffraction peaks of natural montmorillonite, modified montmorillonite and 2 wt% cured nanocomposite. B) TEM image of 2 wt%. cured nanocomposite.

The comparison of XRD patterns of natural montmorillonite, modified montmorillonite [cloisite 30B] and a cured nanocomposite with 2wt.% closite 30B loading is shown in Figure 4-5A. It is difficult to find a prominent peak in a 2 wt.% nanocomposite XRD data. This result can be interpreted by the fact that epoxy resin diffused into galleries and formed intercalated or exfoliated nanocomposite. However, if the nanocomposites are disordered, no peaks are also observed in the XRD, due to loss of the structural registry of the layers, the large d-spacing (>10 nm), or both. Thus, XRD of nanocomposites has limitations because a disordered and layered silicate can either be delaminated or intercalated. In such case transmission electron microscopy (TEM) combined with XRD will more accurately characterize these materials. Instead of showing a prominent peak in a 2 wt.% nanocomposite XRD data, the cured nanocomposite with 2 wt.% clay loading shows a broad and week variance around $2\theta = 2.5°$, $d_{(001)} = 35.34$ Å. If this variance can be interpreted as a peak, TEM image may show ~4 nm gallery spacing. Figure 4-5B shows TEM image of 2 wt.% clay nanocomposite, indicating 3~4 nm gallery spacing. Thus, a weak and broad variance can be interpreted as a peak in XRD data, indicating an intercalated nanocomposite was formed.

Comparing the data in Figure 4-4 and Figure 4-5A, it becomes clear that the cured nanocomposite does not show increased gallery spacing, indicating no further intercalation occurs during the cross-linking reaction. It can be assumed that extragallery curing reaction is faster than intragallery curing reaction. There is no time for a curing

agent to go into the galleries. Therefore, the gallery is not expanded and exfoliation does not proceed.

In this study, nanocomposites were prepared using predetermined rpm (shear force) experiments using a mechanical mixer to investigate the effect of shear force. Impeller speed was varied from 400 rpm to 1000 rpm. Tip velocity of this impeller was calculated using the equation [2].

$$v = \omega \cdot r = RPM \cdot \frac{2\pi}{60} \cdot r \qquad [2]$$

$$\frac{F}{A} = \tau = \mu \cdot \omega \qquad [3]$$

The velocity profile of impeller according to the radius at 1000 rpm was appeared in Figure. It can be predicted that the shear force is linearly proportional to the velocity according to the equation [3].

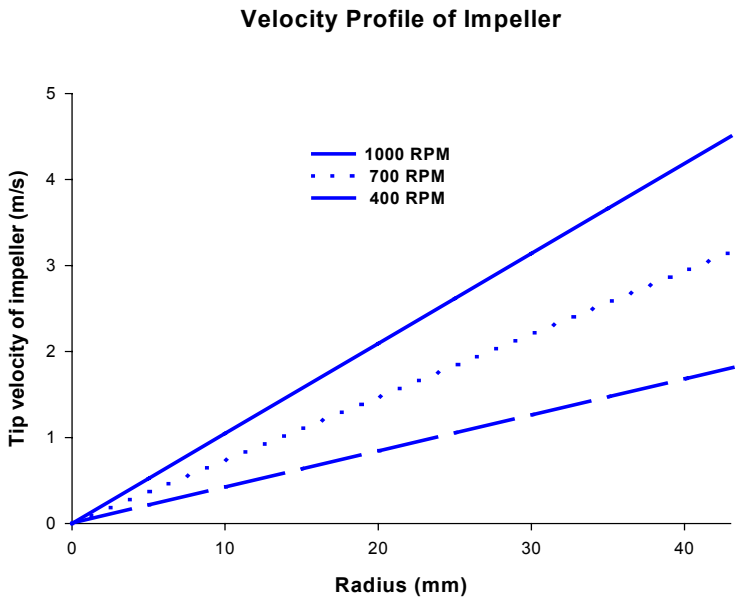

Figure 4-6. The velocity profile Vs Impeller radius.

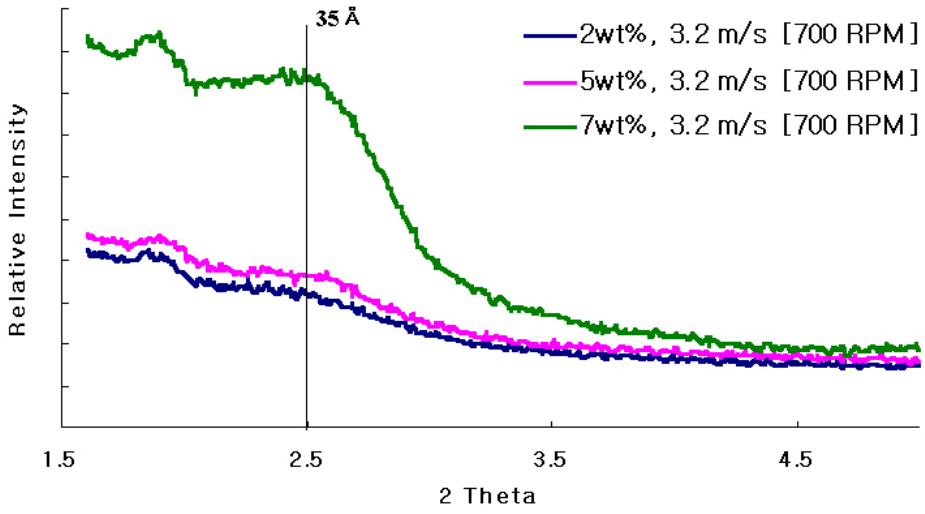

Figure 4-7. The XRD patterns of epoxy-clay nanocomposite were prepared by different clay loadings.

The XRD patterns of different clay contents at fixed tip velocity of impeller (shear force) are observed in Figure 4-7. All three X-ray diffraction patterns of cured nanocomposite containing with 2, 5 and 7 wt.% of clay show similar characteristic diffraction peaks of montmorillonite at around $2\theta = 1.9°$. The broad and weak peaks are appeared at every clay loading nanocomposites at around $2\theta = 2.5°$, $d_{(001)} = 35.34$ Å. This result also shows a sharp increase of intensity with 7 wt.% clay loading nanocomposite. It is assumed that high clay loading may require more shear force to break the clay by decreasing aspect ratio of clay nanoparticle. This broken silicate layer is supported by the increment of the intensity of XRD peak. The results also reveal that the effect of clay loading amounts on the clay basal spacing is not significant.

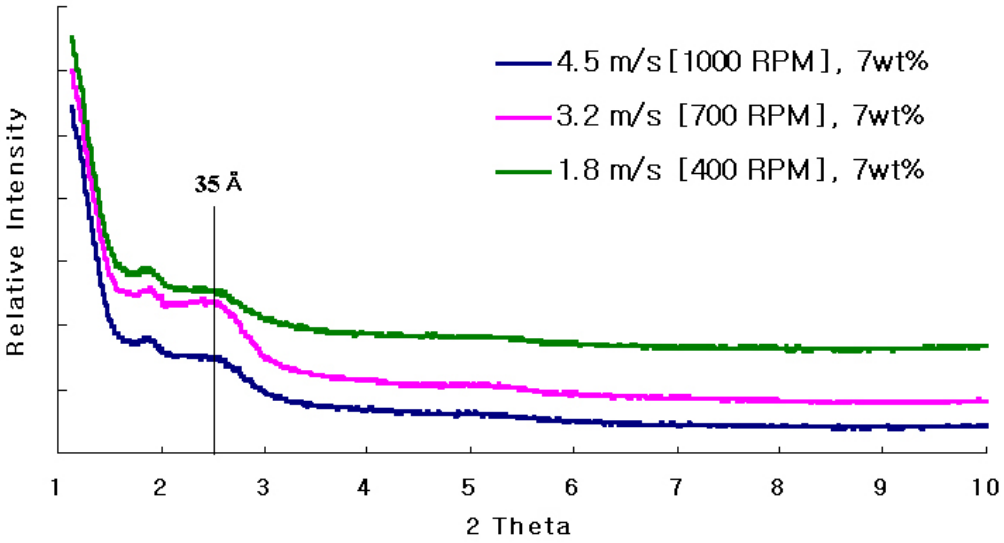

Figure 4-8. The XRD patterns of epoxy-clay nanocomposite were prepared by different shear force (rpm, tip velocity) at the 7wt. % clay loading.

XRD patterns for the epoxy resin/clay/DETDA composite with different rpm processed with 7 wt. percent are shown in Figure 4-8. This also shows a characteristic peak and weak and broad peak intensity change at around $2\theta = 2.5°$, $d_{(001)} = 35.34$ Å. It seems that XRD patterns are not shear force dependent. The peak pattern shows a similar trend at 2 wt.% and 5 wt.% clay loading amount nanocomposites.

To achieve exfoliated nanocomposite, the galleries continue to expand when the degree of polymerization increases and an exfoliated nanocomposite is formed. If the lattice spacing increases further, the diffraction peak will disappear, indicating an exfoliated nanocomposite. If the extragallery polymerization is faster than intragallery polymerization, epoxy monomer cannot enter between the galleries and basal spacing cannot be increased further, thus forming intercalated nanocomposites. It can be assumed that a large amount of epoxy monomer can enter into the gallery by increasing tip velocity (increasing shear force) and the intragallery polymerization can occur at a

comparable rate to extragallery polymerization. However, diffraction peaks of an intercalated nanocomposite are observed. This indicates that the shear forces conducted in this research do not affect the intergallery spacing but rather intergallery spacing is controlled by chemical reaction factor [crosslinking reaction rate] than by mechanical force [shear force].

Figure 4-9 shows XRD patterns of epoxy-clay nanocomposites at different mixing times. The experiment was performed with 5 wt.% clay loading nanocomposits for 24hr and 1 hr mixing times. No significant difference was observed between 24 hr mixing and 1 hr mixing condition, showing also intensity variance around $2\theta = 2.5°$, $d_{(001)} = 35.34$ Å. This increased intensity leads one to believe more silicate layer formed by decreasing aspect ratio of clay. This intensity variance may affect the physical properties of the epoxy-clay nanocomposite. It demonstrates that the mixing conditions could be an important factor while synthesizing the nanocomposite preparation.

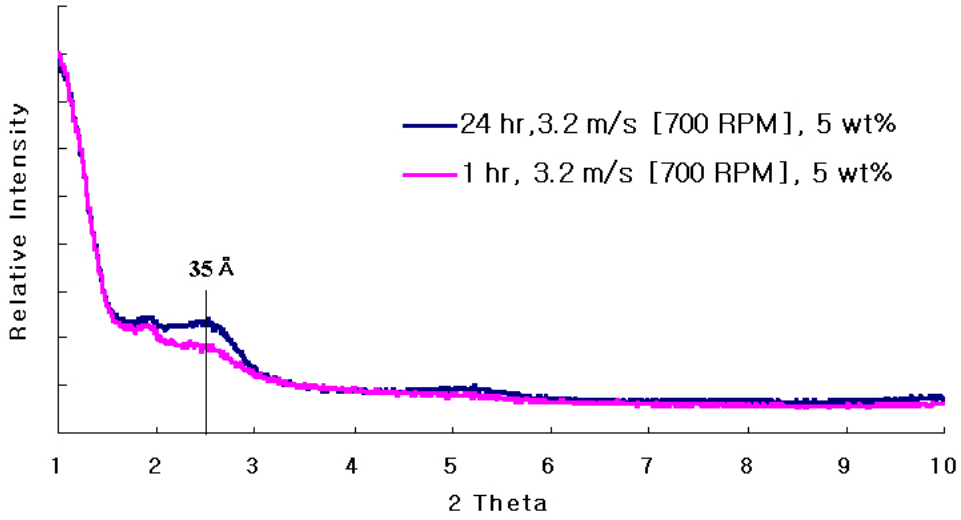

Figure 4-9. Comparison of XRD patterns on different mixing time.

The changes seen in the XRD can be explained by polymer entering the clay galleries pushing the platelets apart (i.e. intercalation). As more polymer chains enter the galleries, two possible changes can occur. First, the platelets can loose their ordered, crystalline structure and become disordered with the platelets no longer parallel without pushing the platelets apart. The result is that the XRD peak broadens into the baseline (intercalated disordered). Secondly, the polymer that enters the galleries pushes the platelets far enough apart that the platelet separation exceeds the sensitivity of XRD (exfoliation). TEM is the better tool to monitor dispersion because the clay platelets can be seen.

Figure 4-10 shows the TEM image of epoxy-clay nanocomposites with stacks of disordered intercalates at high magnification rather than complete exfoliation. The dark lines are the intersections of silicate layers of 1 □ thickness.

Figure 4-10A shows ~4 nm of average distance between clay plates and over 300 □ of the average length of plates for a 2 wt.% hand-mixed processed clay nanocompsite. Figure 4-10B shows ~4 □ of average distance between clay plates and 50 □ of average length of plates for a 5 wt.%, 1000 rpm processed clay nanocomposites. However, X-ray diffraction from these planes does not produce any pronounced peak although the platelets are about 4 nm apart. This could be attributed to either the misalignment or waviness of clay platelets as seen in Figure 4-10.

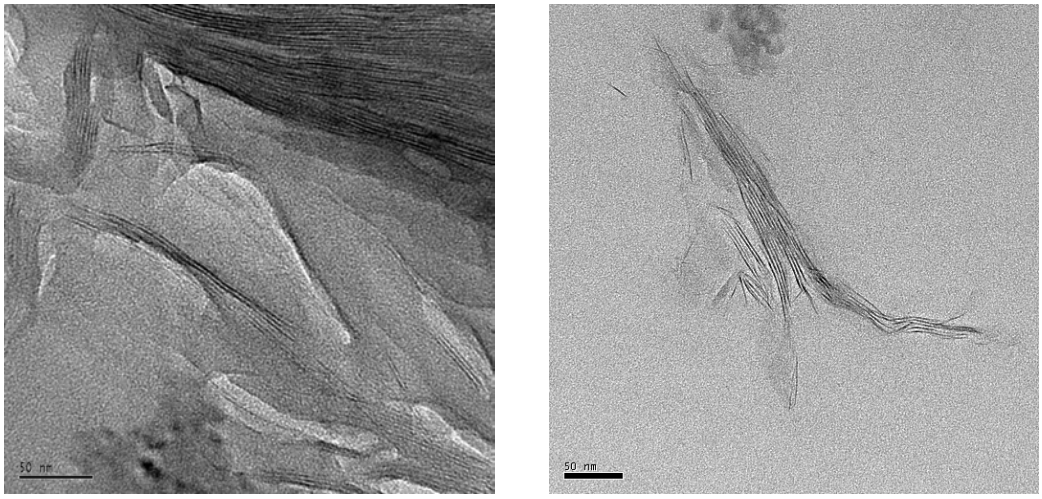

A B

Figure 4-10. TEM images of nanocomposite at high magnification were A) prepared by hand mixing and B) prepared by high shear force (1000 rpm).

Further intercalation / exfoliation didn't occur according to the clay loading or shear forces, but it seems likely that shear forces break clay particles. The aspect ratio of clay plates is reduced from 200~1000 to 10~50 by increasing shear force. Therefore, it can be suggested that this broken clay particle will be dispersed in the epoxy matrix providing more surface area.

The morphology of the composite was examined by a scanning electron microscopy (SEM). Higher shear force induces more evenly distributed clay particles as illustrated in SEM Figure 4-11A, 4-11B, 4-11C and 4-11D. When clay particle were added to the epoxy matrix, the fractured surface became rougher as compared with pristine epoxy (Figure 4-11A). The bright spots correspond to the clay aggregates finely dispersed in the material (Figure 4-11B, C, and D). As shear forces were increased, smaller clay aggregates appeared but were not evenly distributed. Figure 4-11D shows a rougher fracture surface than Figure 4-11B and C. It is expected an even distribution of small particles was achieved by prolonging the mixing time.

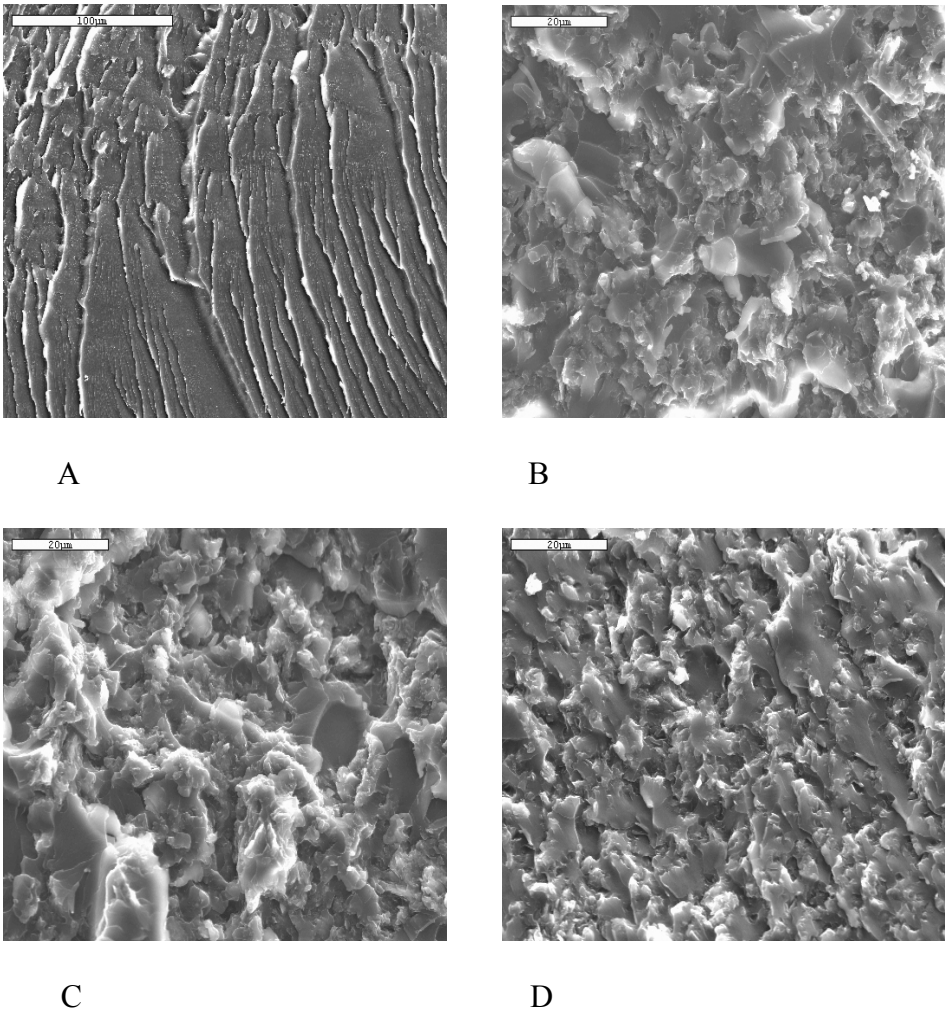

Figure 4-11. The SEM images of fracture surface at A) 0wt%, B) 400 rpm, 5wt%, C) 700 rpm, 5 wt% and D) 24h mixing, 700 rpm, 5 wt%.

Evenly distributed clay particles could be as important as achieving an exfoliated nanocomposite. The smaller clay particles can provide more surface area to prevent the crack propagation. Thus, it can be concluded that mixing time for nanocomposite preparation is also an important processing parameter and these smaller and evenly distributed clay particles increase mechanical properties.

4.2.2 Mechanical Behavior

Mixing clay nanoparticles in an epoxy matrix is expected to improve mechanical properties. Nano-scale clay particle serves a larger surface contact area with the matrix

polymer. Thus, it is anticipated that these silicate layers will prohibit crack propagation. Figure 4-12 shows the stress-strain behaviors of different clay contents hand-mixed (low shear force) nanocomposites under uniaxial tension. As the clay loading amount increases, the tensile strength and the strain to failure decrease. In contrast, the elastic modulus increases with the clay content.

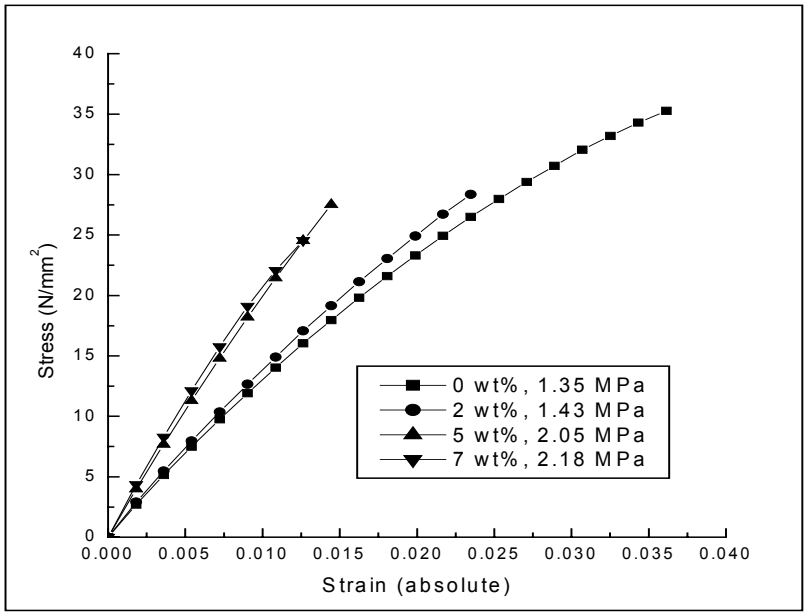

Figure 4-12. Stress-Strain curves of nanocomposites with different wt% clay loading prepared by hand mixing.

In Figure 4-13A, the elastic modulus of the nanocomposites increases continuously with increasing clay content. An improvement of the elastic modulus is continuously increased at the beginning and then the rate of improvement decreases. A direct conclusion from this data is that shear force increases the elastic modulus. The broken and evenly distributed particles have more reinforcement in the nanocomposite which providing blockage to crack propagation.

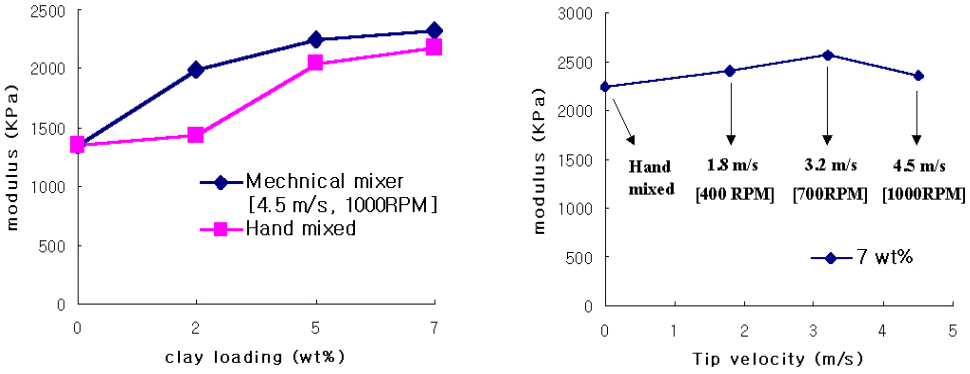

A B

Figure 4-13. The variation of modulus depends on A) clay loading and B) tip velocity of impeller (shear force).

The improvement in elastic modulus can be attributed to the exfoliation and good dispersion of nanosized clay particles that restricts the plastic elastic deformation of polymer chains under loading as well as the good interfacial adhesion between the particles and epoxy matrix. Figure 4-13B shows the variation of elastic modulus with different shear rates at 7 wt.% clay content. This result shows no significant change with increasing shear forces. Although shear force makes smaller clay tactoids by decreasing aspect ratio and increase the number density, it does not dramatically increase the elastic modulus. The longer mixing processed nanocomposite has better mechanical properties because of the evenly distributed small clay aggregates (Figure 4-11D).

4.2.3 Thermal Property

The thermal properties of epoxy-clay nanocomposite were investigated by DSC. Glass transition temperature of nanocomposites with different clay contents at 3.2 ㎧ tip velocity of impeller (700 rpm) is shown in Table 4-1. This table indicates that T_g (glass transition temperature) increases as clay contents increase. This can be explained by the fact that the movements of amorphous epoxy molecular chains are hindered by finely

dispersed clay particles. The thermal properties of epoxy-clay nanocomposites are improved as clay loading increases.

Table 4-1. The T_g variation of nanocomposites prepared with different clay loading.

	T_g (Glass Transition Temperature)
No clay	**99°C**
2 wt.% clay loading	**95.5°C**
5 wt.% clay loading	**102.5°C**
7 wt.% clay loading	**104.5°C**

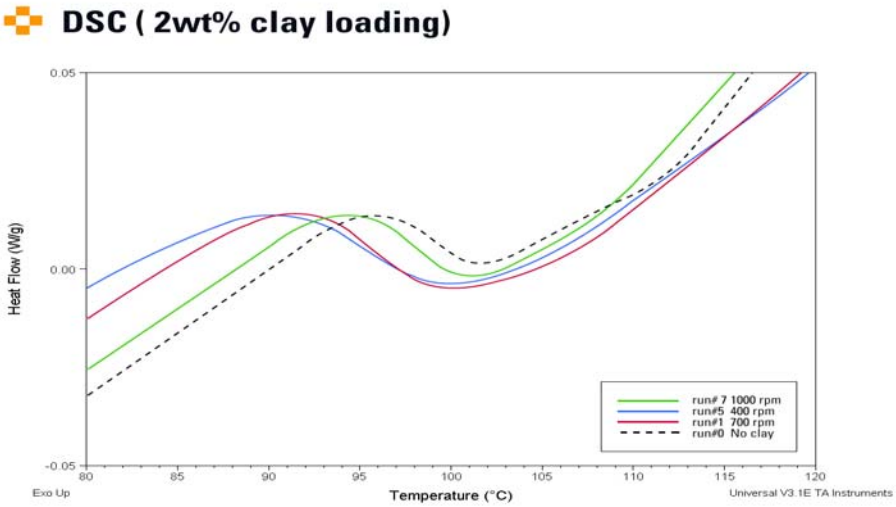

Figure 4-14. DSC data (2 wt% clay loading with different rpm)

Figure 4-14 shows 2 wt% clay loaded samples have lower glass transition temperatures than the no clay loaded sample. Also, lower shear force [1.8 m/s tip velocity] processed sample shows lower glass transition temperature. This could be attributed to the dispersed particle by increasing shear force hinder the heat transfer in the epoxy matrix. Glass transition temperatures of 2wt% clay loaded samples are listed in table 4-2.

Table 4-2. The T_g variation of 2 wt%clay-epoxy nanocomposites with different shear forces.

	T_g (Glass Transition Temperature)
Epoxy Resin	99±3°C
400 rpm (1.8 m/s)	94±4°C
700 rpm (3.2 m/s)	95.5±3°C
1000 rpm (4.5 m/s)	97.5±3°C

We now understand that the mechanical properties and thermal properties of polymer-clay nanocomposites are improved as clay loading increases. Thus, we can expect a higher glass transition temperature as clay-loading increases because movement of amorphous epoxy molecular chain is hindered by finely dispersed clay particles. However, DSC result shows the thermal properties of epoxy/organoclay nanocomposites are not consistently improved as clay loading increases. Figure 4-14 and Table 4-1 show 2 wt% clay loaded samples have lower glass transition temperature than no clay-loaded sample. This means clays in 2 wt% clay loading do not act as filler. Unlike in 2 wt% clay loading samples, clays at 5 wt% and 7 wt% act as filler.

4.2.4 Optical Property

The most significant property of epoxy-layered silicate nanocomposite is their high optical transparency.

Figure 4-15. Transparancy of epoxy-clay [7 wt.% clay loading] nanocomposite.

As shown in Figure 4-15, epoxy-7 wt.% clay loading nanocomposite is almost as transparent as pristine epoxy polymer. The curing agent [diethyltoluenediamine] causes a

yellow tint in the epoxy-clay nanocomposite. This result suggests that the refractive index of the layered silicate mineral family closely matches that of the organic matrix and the small size organo-montmorillonites are uniformly dispersed in the matrix.

CHAPTER 5
CONCLUSION AND FUTURE WORK

Layered silicate clays intercalated by dodecyl-ammonium chloride show increase in intergallery spacing depending on the type of clay minerals. This can be suggested that the cationic surfactant has different arrangements on the clay surface, depending on the different elements and cation exchange capability of clay minerals. The inter-gallery spacing by surface modification can facilitate the entry of epoxy or curing agent molecules to enter into the galleries because the hydrophilic clay surface is changed to an organophilic surface. However, we cannot achieve a completely exfoliated epoxy-clay nanocomposites. This is explained by the fact that the extra-gallery curing reaction is faster than the intra-gallery curing reaction. Therefore, no further curing agents or epoxy resins could enter into the galleries and intercalated epoxy-clay nanocomposite is formed. In this regard, there is no effect due to changing loading amount and shear force. The result reveals that the shear force used in this research does not affect the gallery spacing. Therefore, It suggests that the inter-gallery spacing is affected rather by the chemical reaction than by shear force.

Even though shear force does not lead to an exfoliated nanocomposite, it is found to influence the clay distribution by decreasing the aspect ratio of clay minerals as shown by the TEM analysis revealing the broken silicate layered nanoparticles in the epoxy matrix. Thus, A new model was developed to define the observed result, with modification of Vaia's model as shown in Figure 4-14.

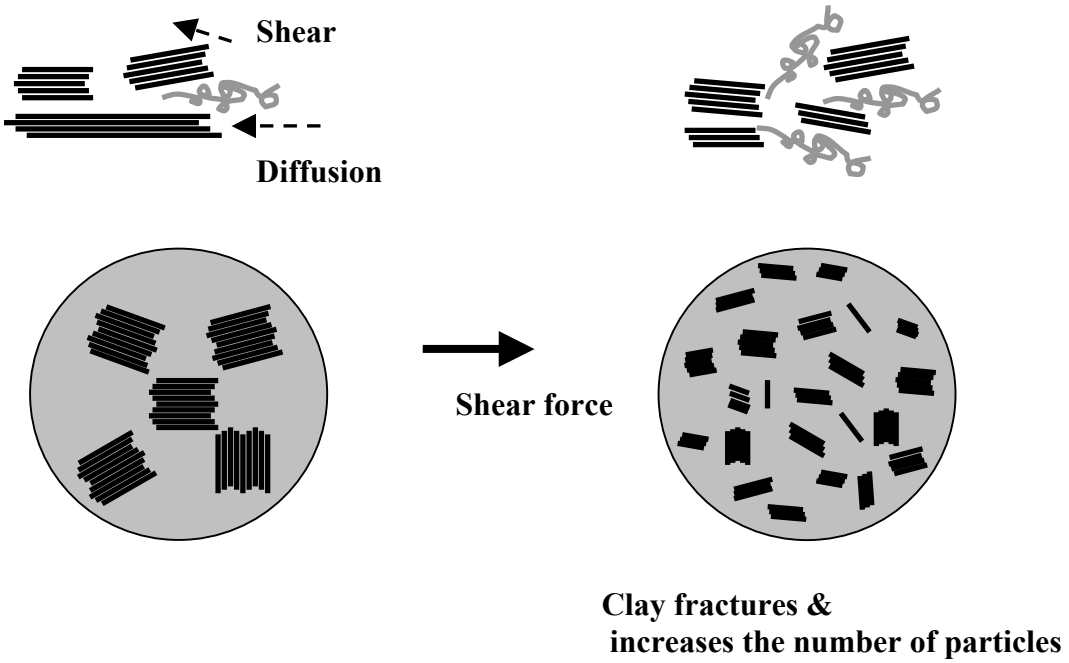

Figure 5-1. Schematic mechanisms of clay platelets intercalation/exfoliation in the epoxy matrix by shear mixing

Vaia assumed the platelet on the top or bottom of a stack is able to bend away from others in the stack as the polymer chains seek to wet or make contact with the organoclay surface. However, this research shows that when shear forces were increased, the organoclay layers have no flexibility and break up, decreasing the aspect ratio, as shown in Figure 4-14. A shear stress is applied, the solution becomes more viscous and the high viscosity increases the stress on the whole tactoids of the organoclay. Although individual aluminosilicate layers are flexible, the applied shear force is felted by the whole tactoids. Thus, these tactoids initially break up and individual layers lose their flexibility to peel apart from stack because of decreased aspect ratio.

Tensile modulus was improved by reinforcing with the clay nanoparticles in an epoxy matrix. The hand-mixed nancomposite shows lower tensile modulus than the nanocomposite formed by mechanical mixing. Thus, the shear force does affect the mechanical properties of the epoxy–clay nanocomosite. This may be explained on the

basis that small tactoids are dispersed in the epoxy matrix and form high surface area. Thus, this dispersed nanoparticle therefore hinders the crack propagation.

Thermal stability is investigated with DSC. As the clay-loading amount is increased, the glass transition temperature also is increased. However, at 2wt.% clay loading amount, the glass transition temperature appears below the epoxy glass transition temperature. This means that a small amount of clay loading can act as impurities in the epoxy matrix. Higher amount of clay loading in the nanocomposite shows good transparency, revealing that modified clays are well dispersed in the epoxy matrix.

The surfactant arrangement in the gallery needs to be further investigated in surface modification on different clay minerals. The difference in gallery spacing is due to the cationic surfactant arrangement, predicting mono-layer or bi-layer formations with different angle arrangement. The understanding of surfactant arrangement in the gallery is necessary for synthesizing advanced epoxy-clay nanocomposites.

The epoxy-clay nanocomposite produced using different shear mixing tools is also need to be investigated. Even though mechanical mixer makes shear force during synthesizing, the shear force used in this research does not affect much the intergallery spacing on the epoxy-clay nanocomposite. Other shear devices that can give more shear force can be utilized to investigate the shear force effect on nanocomposite. Finally, the research about other processing parameters is required to achieve exfoliated epoxy-clay nanocomposite. In this research, we found that the dispersion of clay particle in the epoxy matrix is dependent on the mixing time parameter. It is important that achieving evenly clay particle-dispersed nanocomposite as much as synthesizing exfoliated nanocomposite.

LIST OF REFERENCES

1. Usuki A., Kawasumi M., Kojima Y., Okada A., Kurauchi T., Kamigaito O., J Mater Res., 8, 1174 (1993).

2. Usuki A., Kojima Y., Kawasumi M., Okada A., Fukushima Y., Kurauchi T., Kamigaito O., J Mater Res., 8, 1179 (1993).

3. Kojima Y., Usuki A., Kawasumi M., Okada A., Kurauchi T., Kamigaito O., J Polym Sci, Part A: Polym Chem., 31, 983 (1993).

4. Pinnavaia T. J., Beall G. W., Polymer-Clay Nanocomposite, Jone Wiley & Sons Ltd, Chichester, (2000).

5. Wei-Bing Xu, Su-Ping Bao, Ping-Sheng He, J Appl Polym Sci., 84, 842 (2002).

6. Yano K., Usuki A., Okada A., J Polym Sci, Part A: Polym Chem., 35, 2289 (1997).

7. Tyan H. L., Liu Y. C., Wei K. H., Chem Mater., 11, 1942 (1999).

8. Kornmann X., Berglund L. A., Sterte J., Giannelis E. P., Polym Eng Sci., 38, 1351 (1998).

9. Vaia R. A., Jandt K. D., Kramer E. J., Giannelis E. P., Macromolecules., 28, 8080 (1995).

10. Hasegawa N., Kawasumi M., Kato M., Usuki A., Okada A., J Appl Polym Sci., 63, 137 (1997).

11. Kornmann X., Lindberg H., Berglund L. A., Polymer, 42, 1303 (2001).

12. Chin In-Joo, Thomas Thurn-Albrecht, Kim Ho-Cheol, Thomas P. Russell, Jing Wang, Polymer, 42, 5947 (2001).

13. Salahuddin N, Moet A., Hiltner A., Baer E., European Polym Jour., 38, 1477 (2002).

14. Park Soo-Jin, Seo Dong-Il, Lee Jae-Rock, J. Colloid Interface Sci., 251, 160 (2002).

15. Chen K. H., Yang S. M., J. Appl Polym Sci., 86, 414 (2002).

16. Asma Yasmin, Jandro L. Abot, Issac M. Daniel, Scripta Mater., 49, 81 (2003).

17. Bhattacharya S. K., Tummala R. R., Microelectronics, 32, 11 (2001).

18. Vaia R. A., Jandt K. D., Kramer E. J., Chem Mater., 8, 2628 (1996).

19. Agag T., and Takeichi T., Polymer 41, 7083 (2000).

20. Cho J. W., and Paul D. R., Polymer 42, 1083 (2001).

21. Giannelis E. P., Adv. Mater, 8, 29 (1996).

22. Pinniavaia T. J., Beal G. W., Polymer Clay Nanocomposite, Wiley Series in Polymer Science, London, John Wiley and Sons Ltd, (2000).

23. Vaia R. A., Kishnamoorti R., Polymer Nanocomposites, America Chemical Society Symposium Series 804, London, Oxford University Press. (2001).

24. Yano K., Usuki A., Okada A, Kurauchi T. and Kamigato O., J. Polym. Sci., Part A, Polym. Chem., 31, 2493 (1993).

25. Messersmith P.B. and Giannelis E.P., Chem. Mater., 6,573 (1994).

26. Lan T., and Pinnavaia T. J., Chem. Mater., 6, 2216 (1994).

27. Burnside S. D. and Ginanelis E. P., Chem. Mater., 7, 1597 (1995).

28. Michael Alexandre, Philippe Dubois, Mater Sci. & Eng., 28 (2000).

29. Akelah A., Kelly P., Qutubuddin S. and Moet A., Clay Miner., 29, 169 (1994).

30. Messersmith P.B. and Giannelis E. P., Chem. Mater., 6,1717 (1994).

31. Pinnavaia T. J. and Lan T., Proceedings of the American Society for Composites Eleventh, 558-565 (1996).

32. Kornmann X., Lindberg H. and Berglund L. A., ANTEC'99, 1623-1627 (1999).

33. Wang Z. and Pinnavaia, T. J., Chem. Mater., 10, 1820 (1998).

34. Wei Feng, Abdellatif Ait-Kadi and Bernard Riedl, Polymer Eng. & Sci., 42, 9 (2002).

35. Arimitsu Usuki, Akihiko Koiwai, J App Polym. Sci., 55, 119 (1995).

36. Suh D. J., Lim Y. T., Park O. O., Polymer, 41, 8557 (2000).

37. Tseng Chen-Rui, Wu Jeng-Yue, Polymer, 42, 10063 (2001).

38. Gilman Jeffrey W., Jackson Catheryn L., Chem. Mater. 12, 1866 (2000).

39. Johns W. D. and Sen Gupta P. K., Am. Mineralogist, Vol 52, 1706 (1967).

40. Haase A. J., Weiss A. and Steinfink H., Am. Mineralogist, Vol 48, 261 (1963).

41. Rossman F. Giese, Carel J. Van Oss, Colloid and Surface Properties of Clays and Related Minerals surfactant science series vol. 5., Santa Barbara Science Project, Santa Barbara California.

42. Bailey S. W., Brindley G. W., "Summary of National and International Recommendations on Clay Mineral Nomenclature." 1969-70 CMS Nomenclature Committee. Clays Clay Minerals (1971).

43. Okada A, Kawasumi M, Usuki A, MRS Symposium Proceedings, Pittsburgh, vol. 171; 1990.

44. Giannelis E. P., Adv Mater, 8, 29 (1996).

45. Giannelis E. P., Krishnamoorti R, Manias E, Adv Polym Sci., 138, 107 (1999).

46. LeBaron P. C., Wang Z, Pinnavaia T.J., Appl Clay Sci., 15, 11(1999).

47. Vaia R.A., Price G., Appl Clay Sci., 15, 67 (1999).

48. Biswas M, Sinha Ray S., Adv Polym Sci., 155, 167 (2001).

49. Brindly S.W., Brown G., editors, "Crystal Structure of Clay Minerals and their X-ray Diffraction." London; Mineralogical society,1980.

50. Aranda P., Ruiz-Hitzky E., Chem Mater, 4, 1395 (1992).

51. Greenland D. J., J Colloid Sci., 18, 647 (1963).

52. Blumstein A., J Polym Sci A., 3, 2665 (1965).

53. Krishnamoorti, Vaia R. A., Giannelis E. P., Chem Mater., 8, 1728 (1996).

BIOGRAPHICAL SKETCH

Tak-keun Oh was born in Daegu in Korea on Feburary 26, 1975, to Yongsoo Oh and Jonghyun Park and was raised in Seoul, Korea. After graduating Un-nam high school, he earned a Bachelor of Science degree, with honors, from Han-yang University in Ansan, Korea, in the Department of Metallurgy and Materials Science and Engineering. He then continued his education in pursuit of a master's degree in the Department of Materials Science and Engineering, University of Florida, Gainesville. He has worked at the NSF Engineering Research Center for Particle Science and Technology at the University of Florida for the past 2 years. After graduation, he plans to pursue a Doctor of Philosophy degree in the Department of Materials Science and Engineering, University of Florida